Activation of water by pentavalent actinide dioxide cations: Characteristic curium revealed by a reactivity turn after americium.

Tian Jian[1], Phuong Diem Dau[1], David K. Shuh[1], Monica Vasiliu[2], David A. Dixon[2], Kirk A. Peterson[3], and John K. Gibson[1]*

[1]Chemical Sciences Division, Lawrence Berkeley National Laboratory, Berkeley, California 94720, USA
[2]Department of Chemistry and Biochemistry, University of Alabama, Tuscaloosa, Alabama 35401, USA
[3]Department of Chemistry, Washington State University, Pullman, Washington 99164, USA

*Corresponding author E-mail: jkgibson@lbl.gov

ABSTRACT

Swapping of an oxygen atom of water with that of a pentavalent actinide dioxide cation, AnO_2^+ also called an "actinyl", requires activation of an An-O bond. It was previously found that such oxo-exchange in gas phase occurs for the first two actinyls, PaO_2^+ and UO_2^+, but not the next two, NpO_2^+ and PuO_2^+. The An-O bond dissociation energies (BDEs) decrease from PaO_2^+ to PuO_2^+, such that the observation of a parallel decrease in An-O bond reactivity is intriguing. To elucidate oxo-exchange, we here extend experimental studies to AmO_2^+, americyl(V), and CmO_2^+, curyl(V), which were produced in remarkable abundance by electrospray ionization of Am^{3+} and Cm^{3+} solutions. Like other AnO_2^+, americyl(V) and curyl(V) adsorb up to four waters to form tetrahydrates $AnO_2(H_2O)_4^+$ with the actinide hexacoordinated by oxygens. It was found that AmO_2^+ does not oxo-exchange whereas CmO_2^+ does, establishing a "turn" to increasing reactivity from americyl to curyl, which validates computational predictions. Because oxo-exchange occurs via conversion of an actinyl(V) hydrate, $AnO_2(H_2O)^+$, to an actinide(V) hydroxide, $AnO(OH)_2^+$, it reflects the propensity for actinyl(V) hydrolysis: PaO_2^+ hydrolyzes and oxo-exchanges most easily, despite that it has the highest BDE of all AnO_2^+. A reexamination of computational results for actinyl(V) oxo-exchange reveals distinctive properties and chemistry of Cm(V) species, particularly $CmO(OH)_2^+$.

INTRODUCTION

Gas-phase metal ion reactivity provides insights into metal-mediated chemistry at a fundamental level.[1-8] Particular advantages of actinide (An) ion chemistry in the gas phase include sample sizes of $<10^{-6}$ g, which enables experiments using radioactive and scarce transplutonium isotopes such as ^{243}Am (half-life $7.4x10^3$ y) and ^{248}Cm ($3.4x10^5$ y). Also, gas-phase phase species produced by electrospray ionization (ESI) and collision induced dissociation may exhibit unusual structures and bonding motifs that can elucidate essential chemistry.[9] In the gas phase, the species are free from perturbations from neighboring molecules or solvents and that can reveal characteristics and trends that may otherwise be obscured by complexities of condensed phases. However, this does not exclude electronic perturbations in individual molecules from other close lying electronic states. In essence, actinide chemistry in the gas phase provides a foundation to better understand more complex and sometimes inscrutable phenomena in solids and liquids.

The ability of bare and ligated actinide cations to activate simple molecules has illuminated actinide-oxo ligand bonding and reactivity in both condensed and gas phases.[10-19] Among species of particular interest are the so-called actinyl ions, $An^{V}O_2^+$ and $An^{VI}O_2^{2+}$, which have distinctive linear O_{YL}=An=O_{YL} structures.[20-22] The general phenomenon of exchange of the oxygen atom in a water molecule with an oxygen atom in a metal complex, so-called oxo-exchange, provides evidence for activation of the metal oxide bond via water deprotonation and metal hydroxlation.[23] Oxo-exchange reactions of bare actinyl(V) ions can be tracked using isotopes ^{16}O and ^{18}O, as in reaction (1).

$$\mathbf{An^{16}O_2^+ + H_2{}^{18}O \rightarrow An^{16}O^{18}O^+ + H_2{}^{16}O} \quad \mathbf{(1)}$$

Although oxo-exchange involves no net chemical change, it requires activation of an An-^{16}O bond to ultimately yield An-^{18}O, a phenomenon that has been studied in solution.[24-25] An appeal of gas-phase reaction (1) is the elementary and unambiguous mechanism given by the potential energy surface (PES) in Figure 1.[26] A key step is conversion of the physisorption hydrate, $AnO_2(H_2O)^+$, via the proton-transfer transition state, *TS-PT*, to the chemisorption hydroxide, $AnO(OH)_2^+$. For all $AnO(OH)_2^+$ except for An = Pa and Cm, the two hydroxyl groups are non-equivalent, one being quasi-axial, $(OH)_{AX}$, and the other quasi-equatorial, $(OH)_{EQ}$, with respect to the terminal oxo-group. Oxo-exchange proceeds via the hydroxide transition state, *TS-OH*, in which the hydroxyl groups are equivalent. Exchange is completed by retracing the PES back from *TS-OH* to the reactants, but with the ^{16}O and ^{18}O labelled atoms swapped (Figure S1). Bimolecular

oxo-exchange reaction (1) under thermal conditions should occur if both *TS-PT* and *TS-OH* lie below the energy asymptote (E≡0) defined by the separated reactants; exchange cannot occur if either *TS* energy is above E≡0.

It was previously reported that oxo-exchange reaction (1) is faster for UO_2^+ than NpO_2^+ and PuO_2^+, which seemed enigmatic because the bond dissociation energy (BDE) is higher for U-O than Np-O and Pu-O.[26] The energies computed by density functional theory for *TS-PT* were in accord with observations—E[*TS-PT*] for UO_2^+ is lower than for NpO_2^+ and PuO_2^+—but did not reveal underlying origins for the differences in reactivity. It was later demonstrated that PaO_2^+, which has the highest BDE of all AnO_2^+, exchanges even more efficiently than UO_2^+.[27] The Pa results also revealed unusual stability of hydrolyzed Pa(V) relative to hydrated protactinyl(V), which is in accord with solution behavior.[28] Recent coupled cluster (CCSD(T)) calculations indicate that all nine actinide dioxides from PaO_2^+ to EsO_2^+ are actinyl(V) species, $[O_{YL}=An^{V}=O_{YL}]^+$.[29-30] It should be noted that it was initially reported that CmO_2^+ is a Cm^{III} peroxide rather than a Cm^{V} actinyl.[29] However, this characterization was subsequently revised by the same authors, with $[O_{YL}=Cm^{V}=O_{YL}]^+$, curyl(V), ultimately identified as the definitively lowest energy structure.[30] Prior to identification of bare curyl(V) the only known Cm(V) species was anion complex $CmO_2(NO_3)_2^-$ in which a CmO_2^+ moiety is coordinated by two nitrate anions.[31]

The CCSD(T) results predict that oxo-exchange should not occur for AmO_2^+, but should occur for CmO_2^+, BkO_2^+, CfO_2^+ and EsO_2^+,[30] which presents opportunities to assess the validity of the computational results, as well as to further evaluate underlying properties that govern differences in reactivity. Americyl(V) and curyl(V) are obvious experimental targets, following along the lines of previous studies of oxo-exchange for the first four actinyl(V), PaO_2^+, UO_2^+, NpO_2^+ and PuO_2^+.[26-27] The CCSD(T) prediction that AmO_2^+ should not oxo-exchange is remarkable because the Am-O BDE is ~300 kJ/mol lower than the U-O BDE in UO_2^+; americyl(V) is a test case for the unimportance of bond strength in inhibiting oxo-exchange. The particular significance of CmO_2^+, curyl(V), is the prediction of a distinct shift from continually decreasing oxo-exchange reactivity from PaO_2^+ to AmO_2^+, turning to higher reactivity from AmO_2^+ to CmO_2^+. Particular challenges in the proposed transplutonium oxo-exchange studies, beyond increasing radionuclide handling constraints for the relatively short-lived available isotopes, are synthesis of bare gas-phase actinyl(V), particularly curyl(V) which is predicted to be marginally stable with an estimated BDE[OCm^+-O] of only 202±60 kJ mol^{-1}.[32]

Reported here are results for reactions of $^{243}Am^{16}O_2^+$ and $^{248}Cm^{16}O_2^+$ with $H_2{}^{18}O$, studied in a quadrupole ion trap mass spectrometer (QIT-MS). The bare americyl(V) and curyl(V) cations were produced in remarkable abundance by ESI of solutions containing Am^{3+} and Cm^{3+}. The key finding is that, under thermal conditions (~300 K), AmO_2^+ does not oxo-exchange with water, whereas CmO_2^+ does. The results are discussed in the context of trends across the series of actinyl(V) ions, with a central conclusion that Cm(V) is idiosyncratic. It is also shown that AmO^+ exhibits rapid oxo-exchange; because the Am-O BDE for AmO^+ is higher than for AmO_2^+, which does not oxo-exchange, this result and comparison further demonstrates unimportance of bond strength in governing this oxo-bond activation.

EXPERIMENTAL

Caution! The Am-243 and Cm-248 isotopes employed in this work are highly radiotoxic and must be handled only in special radiological laboratories.

The experiments were performed using an Agilent 6340 QIT-MS with the ESI source inside a radiological contaminant glovebox as described previously.[33] Oxide cations AmO^+, AmO_2^+, CmO^+ and CmO_2^+ were produced by ESI using ethanol solutions containing ~200 μM $^{243}AmCl_3$, $^{243}Am(ClO_4)_3$, or $^{248}CmCl_3$. The QIT has been modified to allow for introduction of reagent gases through a gas manifold and leak valve. Ions in the trap can undergo ion-molecules reactions for times in the range 0.05 s to 10 s at ~300 K.[34] Mass spectra were acquired in the positive ion accumulation and detection mode using the following parameters: solution flow rate, 60 μL/h; nebulizer gas pressure, 15 psi; capillary voltage offset and current, -4500 V and 30.518 nA; end plate voltage offset and current, -500 V and 175.000 nA; dry gas flow rate, 2 L/min; dry gas temperature, 325 °C; capillary exit, 147.3 V; skimmer, 40.0 V; octopole 1 and 2 DC, 12.00 V and 3.67 V; octopole RF amplitude, 200.0 V_{pp}; lens 1 and 2, -5.0 and 12.00 V; trap drive, 180.4. Nitrogen gas for nebulization and drying was supplied from the boil-off of a liquid nitrogen reservoir. Helium buffer gas pressure in the trap is constant at $\sim 1\times10^{-4}$ torr, and background water pressure in the ion trap is estimated as $\sim 1\times10^{-6}$ torr.[35] Reproducibility of hydration kinetics for $UO_2(OH)^+$ established that the background water pressure does not vary by more than 20%. Isotopically labelled $H_2{}^{18}O$ (Aldrich, 99% ^{18}O) was admitted to the ion trap through a leak valve. Oxo-exchange of $U^{16}O_2(^{16}OH)^+$ with $H_2{}^{18}O$ is sufficiently fast that equilibrium is achieved in ≤0.05 s, with the resultant $U^{16}O_2(^{18}OH)^+$/ $U^{16}O_2(^{16}OH)^+$ ratio providing the $H_2{}^{18}O/H_2{}^{16}O$ pressure

ratio.[26] For some experiments, acetone was added to the QIT at a pressure estimated as roughly comparable to that of water, ~1×10^{-6} torr.[33]

RESULTS AND DISCUSSION

Preparation and hydration of AmO^+, AmO_2^+, CmO^+ and CmO_2^+

ESI mass spectra for Am^{3+} and Cm^{3+} solutions are shown in Figure 2. Similar results were obtained for the chloride and perchlorate solutions of Am^{3+}. Also shown is an ESI mass spectrum obtained under similar conditions for a U(VI) chloride solution. The uranium results are typical for ESI of U(VI): the dominant gas-phase species is uranyl(V), UO_2^+, with a smaller yield of U(VI) as $UO_2(OH)^+$. UO_2^+ is very stable, as indicated by the BDEs in Table 1. AmO_2^+ and CmO_2^+ are much less stable, with a result that along with Am(V) and Cm(V) species from ESI there is a substantial abundance of $Am^{III}O^+$ and $Cm^{III}O^+$. The appearance of appreciable AmO_2^+ and CmO_2^+ under these conditions is remarkable given their limited stabilities, particularly for the latter. Whereas gas-phase AmO_2^+ has been prepared by oxidation of AmO^+ by ethylene oxide under thermal conditions,[36] only excited state CmO^+ reacted with O_2 to produce CmO_2^+.[37] A feasible route to formation of AnO_2^+ under relatively high pressure ESI conditions is association of An^+ and O_2. The reaction of CmO^+ with O_2 to yield CmO_2^+ (and atomic O) is endothermic by ~300 kJ/mol, but association of Cm^+ with O_2 to yield CmO_2^+ is exothermic by ~370 kJ/mol. The Am(V) and Cm(V) species observed in the ESI mass spectra of Am^{3+} and Cm^{3+} solutions are a demonstration that gas-phase ions produced by this approach do not necessarily reveal solution speciation. In contrast to well established Am(V) in solids and solutions, pentavalent curium in condensed phase has not been reported and is likely unstable;[38] the observation here of Cm(V) in gas phase does not indicate the presence of this oxidation state in the precursor solution. Nor does the appearance of the small peak in Figure 2b due to Am^+ indicate the presence of Am(I) in solution.

Before studying oxo-exchange using $H_2{}^{18}O$ added to the ion trap, simple water addition reactions were examined using natural background H_2O (>99.5% $H_2{}^{16}O$). Results for reactions of UO_2^+, AmO_2^+ and CmO_2^+ with background gases in the ion trap are shown in Figure 3. The results for UO_2^+ are essentially the same as reported previously. UO_2^+, like NpO_2^+ and PuO_2^+, adsorbs up to four water molecules to yield tetrahydrate $UO_2(H_2O)_4^+$.[39] Under these conditions (<10^{-3} Torr, 300 K) only waters that bind directly to the actinide center—i.e. inner-sphere oxo-coordination—

are adsorbed, such that in $AnO_2(H_2O)_4^+$ the four ligated waters bind to the An center. In contrast to NpO_2^+ and PuO_2^+, uranyl(V) can oxidatively adsorb background O_2 to yield $UO_2(O_2)(H_2O)_3^+$, a U(VI) superoxide. Adsorbing up to four waters with no detectable O_2 addition, AmO_2^+ and CmO_2^+ exhibit typical actinyl(V) hydration. As for Np and Pu, oxidation to Am(VI) or Cm(VI) by O_2 is not observed.

Relative rates for addition of the first water to AnO_2^+ can be estimated from the aggregate yield of primary $AnO_2(H_2O)^+$ and all secondary and higher order products that form via the primary hydrate. The results in Figure 3 suggest that the rate of water addition is similar for UO_2^+ and CmO_2^+, and ~30% slower for AmO_2^+. However, the key result is not this relatively small rate difference but rather that these three AnO_2^+, like NpO_2^+ and PuO_2^+, add up to four waters and do so with qualitatively similar kinetics. In contrast, under comparable conditions to those used for the results in Figure 3, PaO_2^+ exhibits rather different hydration kinetics. Most notably, under conditions where intermediate hydrates such as $AnO_2(H_2O)_3^+$ (An = U, Np, Pu, Am, Cm) are abundant, such as in Figure 3, only unreacted PaO_2^+ and fully hydrated $PaO_2(H_2O)_4^+$ are significant. The essentially disparate hydration kinetics of PaO_2^+ is attributed to the distinctive propensity for facile hydrolytic isomerization of hydrate $PaO_2(H_2O)^+$ to hydroxide $PaO(OH)_2^+$, which then efficiently adds waters of hydration. The hydration kinetics apparent in Figure 3 thus suggest that AmO_2^+ and CmO_2^+, like UO_2^+, physisorb water to yield hydrates, $AnO_2(H_2O)^+$, rather than hydroxides, $AnO(OH)_2^+$.

In addition to different hydration kinetics, the different coordination chemistries of gas-phase hydrates and isomeric hydroxides can distinguish them. The physisorbed water molecule in $AnO_2(H_2O)^+$ is displaced by a stronger gas-phase base such as acetone (aco).[40] In contrast, chemisorbed hydroxyl groups in the alternative $AnO(OH)_2^+$ isomer are not displaced by a datively coordinating Lewis base ligand like aco. This ligand-displacement approach was previously demonstrated for thorium and protactinium hydrates/hydroxides,[27, 41] including differentiation of $PaO_2(H_2O)^+$ from $PaO(OH)_2^+$. The results for reaction of $AmO_2(H_2O)_2(aco)^+$ with aco (Figure S2a) show that both water molecules are displaced to yield $AmO_2(aco)_3^+$ which indicates physisorption of water by AmO_2^+ to yield hydrate $AmO_2(H_2O)^+$, rather than hydroxide $AmO(OH)_2^+$. The hydrate structure was also inferred above based on hydration kinetics. In contrast to AmO_2^+, the water adduct to AmO^+ reacted with aco by addition, rather than water-displacement (Figure S2b), which indicates that the formulation is as the hydroxide $Am(OH)_2^+$, rather than the hydrate, $AmO(H_2O)^+$.

Based on gas-phase reactions with aco, we conclude that a water molecule physisorbs to AmO_2^+ to yield $AmO_2(H_2O)^+$, and chemisorbs to AmO^+ to yield $Am(OH)_2^+$.

Results for water addition to AmO^+ and CmO^+ are shown in Figure S3. Both of these AnO^+ exhibit similar behavior, adsorbing four water molecules to yield $AnO(H_2O)_4^+$; as discussed above, the more plausible formulation is as $Am(OH)_2(H_2O)_3^+$ (and thus also likely as $Cm(OH)_2(H_2O)_3^+$). Although the abundances are low, there is convincing evidence in Figure S3 for inefficient addition of a fifth water to yield $Am(OH)_2(H_2O)_4^+$ and $Cm(OH)_2(H_2O)_4^+$, in which there is net actinide hexacoordination, this being the same overall coordination as in the actinyl tetrahydrates $AnO_2(H_2O)_4^+$.

Oxo-exchange by americium and curium oxide cations

The results discussed above show that AmO_2^+ and CmO_2^+ produced by ESI exhibit essentially the same hydration behavior as other actinyls such as NpO_2^+ and PuO_2^+. This accord substantiates the premise that americyl(V) and curyl(V) have been prepared such that their oxo-exchange can be reliably assessed. The results in Figures 3 and S7 demonstrate that, like $U^{16}O_2^+$, neither $Am^{16}O_2^+$ nor $Cm^{16}O_2^+$ react with $H_2{}^{16}O$ or other background gases to yield $An^{16}O_2H_2^+$ that would not be differentiated with our mass spectrometer from isobaric oxo-exchange product $An^{16}O^{18}O^+$.

In Figure 4 are presented results for reaction of $U^{16}O_2^+$ and $Am^{16}O_2^+$ with the same pressure (to within 10%) of $H_2{}^{18}O$ for 1 s and 10 s, respectively. In accord with previous results, it is apparent in Figure 4 that uranyl oxo-exchanges with water to yield $U^{16}O^{18}O^+$. Even for the 10 times longer reaction time, no detectable $Am^{16}O^{18}O^+$ is produced. Based on the estimated $Am^{16}O^{18}O^+$ detection limit (~2%) and the yield of $U^{16}O^{18}O^+$ (10%) we conclude that undetected oxo-exchange for AmO_2^+ is at least 500 times slower than for UO_2^+.

The results for oxo-exchange of $U^{16}O_2^+$ and $Cm^{16}O_2^+$ at nearly the same $H_2{}^{18}O$ pressure and for the same reaction time are shown in Figure 5. Both UO_2^+ and CmO_2^+ exchange under these conditions. From the relative product yields, it is apparent that uranyl(V) exchanges roughly twice as efficiently as curyl(V). In Figure S4 the expected increasing oxo-exchange yield for CmO_2^+ with increasing reaction time is apparent. However, for times longer than ~2 s the relative background ion intensities become too high for reliable determination of products.

In contrast to earlier actinides, Pa, U, Np and Pu, which form mainly An(V) species in ESI, there are substantial ESI yields of Am(III) and Cm(III) monoxide cations, AnO^+, which reflects

relatively low OAn^+-O BDEs for Am and Cm (Table 1). Oxo-exchange was studied for $Am^{16}O^+$ and $Cm^{16}O^+$ with $H_2{}^{18}O$ at roughly the same pressure as used with the $An^{16}O_2^+$. The results (Figures S5 and S6) show that both $Am^{16}O^+$ and $Cm^{16}O^+$ exchange so fast, as does the hydroxyl group of $UO_2(OH)^+$, that exchange equilibrium is achieved within 0.05 s, the shortest reaction time accessible in these experiments. Comparison with the above results for actinyl(V) reveals that AmO^+ and CmO^+ exchange at least 10^4 times faster than the corresponding AnO_2^+. Referring to Table 1, the An-O BDEs are substantially higher for the monoxide versus dioxide cations, particularly for CmO^+ (BDE[Cm^+-O ≈ 670 kJ/mol) versus CmO_2^+ (OCm^+-O ≈ 202 kJ/mol). The result that the two AnO^+ oxo-exchange much faster than the corresponding AnO_2^+ demonstrates that this bond activation is not directly governed by the energy for An-O bond cleavage. As discussed below, it is not necessarily incongruous that stronger bonds exhibit more facile activation.

Assessment of CCSD(T) computational predictions

The new experimental results for oxo-exchange of AmO_2^+ and CmO_2^+ invite assessment of previous CCSD(T) computations of the PES in Figure 1, which were reported for all actinyl(V), PaO_2^+ to EsO_2^+.[30] For consistency, all previously reported parameters that are re-considered here are specifically at theory level CCSD(T)/awT-DK3 (PW91).[30]

Validation of PES energies; revisiting the reactivity "enigma"

Under low-energy experimental conditions, bimolecular reaction (1) can occur only if all energies on the PES are below (or at) the reactant energy asymptote (E≡0). The highest energy on each PES is *TS-PT* or *TS-OH*; the latter is higher in energy only for AmO_2^+ and CfO_2^+ (see Figure S8). Because for AmO_2^+ and CfO_2^+ the prediction of whether exchange should occur—it should not for AmO_2^+ and it should for CfO_2^+—is the same whether considering *TS-PT* or *TS-OH*, we simplify the discussion by considering only *TS-PT* for all AnO_2^+. The computed E[*TS-PT*] are plotted in Figure 6 together with other selected PES energies. The CCSD(T) predictions that PaO_2^+ and UO_2^+ should exchange (i.e. E[*TS-PT*] < 0), whereas NpO_2^+ and PuO_2^+ should not exchange (i.e. E[*TS-PT*] > 0)[30, 42], were experimentally established.[26-27] We have now verified the genuinely predictive CCSD(T) results that AmO_2^+ should not exchange and CmO_2^+ should. The accuracy of these predictions supports trends in computed energies and provides overall confidence.

The apparent enigma of more facile activation of stronger bonds is exemplified by the increase in E[hydrate → *TS-PT*] from PaO_2^+ to AmO_2^+, concurrent with a decrease in bond

strength, as indicated by both the computed (Fig. S9) and experimental (Table 1) BDE[OAn^+-O]. In contrast to the barrier for transformation of the hydrate to hydroxide, the reverse barrier for conversion of hydroxide to hydrate, E[hydroxide → *TS-PT*], decreases from PaO_2^+ to AmO_2^+ (Figure 6). Like BDE[OAn^+-O], the BDE of hydroxide An-OH bonds, BDE[OAn^+-$(OH)_2$] as defined in Figure S9, also decreases from PaO_2^+ to AmO_2^+. The BDE to cleave two An^V-(OH) bonds is consistently greater than, though nowhere near twice as great as, the energy to cleave one An^V-O_{YL} bond, with the magnitude of this difference directly reflecting the relative hydrolysis energies: the greater the hydrolysis energy, the higher is the BDE for An-O_{YL} relative to An-(OH). Because E[hydroxide → *TS-PT*] and BDE[OAn^+-$(OH)_2$] decrease in parallel with one another, from the perspective of activation of An-OH bonds, there is no enigma of more facile activation of stronger bonds.

A more general consideration for resolving the apparent enigma of more facile activation of stronger actinyl bonds is that at no point in the transformation of $AnO_2(H_2O)^+$ to $AnO(OH)_2^+$ via *TS-PT*, as well as in the reverse transformation, is an An-O bond actually severed. Accordingly, there should not necessarily be a correlation between such activation and bond strength as indicated by BDE for bond cleavage. It is concluded that it is really not enigmatic that the barrier for conversion of An-O_{YL} and An-(H_2O) bonds to two An-(OH) bonds, via *TS-PT* in which none of the An-O bonds are fully destroyed, should not depend on the absolute bond energies. As elaborated below, the energy difference between the hydrate and hydroxide is more pertinent to the proton-transfer barrier *TS-PT* than are the absolute bond energies for either.

The computed hydrolysis energies in Figure 6 provide relative stabilities of the hydrate and hydroxide as ΔH(hydrolysis). The prediction that the Pa hydrate and hydroxide isomers are similar in energy (ΔH(hydrolysis) ≈ -3 kJ/mol) was previously confirmed from coexistence of $PaO_2(H_2O)^+$ and $PaO(OH)_2^+$.[27] For all other AnO_2^+, hydrolysis is computed to be substantially endothermic, specifically by 198 kJ/mol for AmO_2^+ and 121 kJ/mol for CmO_2^+.[30] The acetone replacement results above demonstrated that water addition to AmO_2^+ yields $AmO_2(H_2O)^+$, not $AmO(OH)_2^+$, in accord with the computed higher stability of the hydrate. Hydration kinetics furthermore support formulation as $CmO_2(H_2O)^+$ rather than $CmO(OH)_2^+$, also in accord with computed energies. As for oxo-exchange, the experimental results indicating hydration rather than hydrolysis support the computational predictions.

Distinctive curium(V)

The relationships for E[*TS-PT*] given by equations (2a) and (2b) follow directly from the PES in Figure 1. It is apparent in Figure 6 that E[*TS-PT*] correlates with barrier E[hydrate → *TS-PT*]. This correlation reflects that the difference between these two energies is the hydration energy ΔH(hydration), which is roughly -150 kJ/mol and varies by less than 23 kJ/mol from PaO_2^+ to CmO_2^+. It should be noted that the variation in ΔH(hydration) is somewhat greater (46 kJ/mol) from BkO_2^+ to EsO_2^+, but the focus here is from PaO_2^+ to CmO_2^+.

$$\mathbf{E[\mathit{TS}\text{-}\mathit{PT}] = \Delta H(hydration) + E[hydrate \rightarrow \mathit{TS}\text{-}\mathit{PT}]} \quad \mathbf{(2a)}$$

$$\mathbf{E[\mathit{TS}\text{-}\mathit{PT}] = \Delta H(hydration) + \Delta H(hydrolysis) + E[hydroxide \rightarrow \mathit{TS}\text{-}\mathit{PT}]} \quad \mathbf{(2b)}$$

Also apparent in Figure 6 is a general correlation between E[*TS-PT*] and ΔH(hydrolysis). This relationship reflects equation (2b), where E[*TS-PT*] is the sum of ΔH(hydrolysis) and E[hydroxide → *TS-PT*], modified by the nearly constant ΔH(hydration). For PaO_2^+ to CmO_2^+, variations in ΔH(hydrolysis) are greater than those in E[hydroxide → *TS-PT*], such that E[*TS-PT*], the observable barrier to gas-phase oxo-exchange, is practically governed by the hydrolysis energy. Accordingly, among the first six actinyl(V), PaO_2^+ has the lowest ΔH(hydrolysis) and E[*TS-PT*] (-3 and -29 kJ/mol, respectively), while AmO_2^+ has the highest of both (150 kJ/mol and 57 kJ/mol, respectively).

Not only is there a "turn" to lower E[*TS-PT*] from AmO_2^+ to CmO_2^+, but in comparison with other neighboring AnO_2^+, the decrease there is also especially large (from 57 for AmO_2^+ to -14 kJ/mol for CmO_2^+, Figure 6); this reflects the distinctive and additive decreases from AmO_2^+ to CmO_2^+ in both quantities ΔH(hydrolysis) and E[hydroxide → *TS-PT*] that appear in equation (2b). This intriguing characteristic "turn" from Am(V) to Cm(V) can thus be understood from trends for PES energies in Figure 6. The endothermic energy of hydrolysis increases from Pa to Am. According to Hammond's Postulate,[43] for a more endothermic hydrolysis reaction *TS-PT* should be more similar to the products such that the barrier E[hydrate → *TS-PT*] should be higher, which is just as seen in Figure 6 from Pa to Am. As expected from Hammond's Postulate, as ΔH(hydrolysis) decreases from Am to Cm, so does E[hydrate → *TS-PT*].

While the barrier E[hydrate → *TS-PT*] increases from Pa to Am, the reverse barrier E[hydroxide → *TS-PT*] decreases, which is just as expected from Hammond's Postulate because *TS-PT* is expected to become more similar to the hydroxide from Pa to Am. An apparent contradiction is the decrease from Am to Cm in E[hydroxide → *TS-PT*], in parallel with a decrease

in E[hydrate → *TS-PT*]. This inconsistency, which essentially accounts for the drastic decrease in E[*TS-PT*] from Am to Cm, suggests underlying distinctive chemistry for one or more of the curium species on the PES.

A direct result of the distinctively large decrease in E[*TS-PT*] from AmO_2^+ to CmO_2^+ is the linked predictions that AmO_2^+ should not exchange while CmO_2^+ should. A particularly important result of the present experimental study is confirmation of this prediction, and, thus, also of a characteristic sharp turn in reactivity between americyl(V) and curyl(V).

The striking decrease in oxo-exchange reactivity between americyl(V) and curyl(V) is intriguing. As discussed above, it is evidently the higher reactivity of CmO_2^+ that is idiosyncratic, which may suggest peculiar characteristics for this species and/or other curium species on the PES. Notably, BDE[OAn^+-O] is a minimum for CmO_2^+ (Table 1 and Figure S9), and the curyl(V) structure, $[O=Cm^{V}=O]^+$, is only 46 kJ/mol lower energy than the curium(III) peroxide structure, $[Cm^{III}(\eta^2\text{-}O_2)]^+$. The stability of the $An^{V}O(OH)_2^+$ also exhibits a minimum at Cm, as indicated by the BDE values plotted in Figure S9. The decrease in stability of the pentavalent oxidation state from Pa to later actinides is well established.[44] The particularly high stability of the trivalent oxidation state of curium is generally attributed to the energy benefit provided by the half-filled f subshell in the electronic configuration of Cm^{3+}, $[Rn]5f^7 6d^0 7s^0$. Another result of the high stability of Cm(III) is relatively low stabilities of higher oxidation states such as Cm(V), which is unknown in condensed phases.[45]

Distinctive character of some Cm(V) species on the PES is also revealed by trends in computed bond distances derived from reported B3LYP geometrical parameters (see SI).[30] In Figure 7 are plotted the distances for An-$(OH)_{AX}$, An-$(OH)_{EQ}$ and An-O_T in $AnO(OH)_2^+$, and for An-O_{YL} in $AnO_2(H_2O)^+$. Although variations in An-O_{YL} are rather small, there is a slight, but not particularly remarkable, increase in this particular parameter from $AmO_2(H_2O)^+$ to $CmO_2(H_2O)^+$. Much more conspicuous deviations appear for the three actinide-oxygen distances in $AnO(OH)_2^+$, all of which exhibit distinct maxima at An=Cm. Although the An-(OH) BDEs for $AnO(OH)_2^+$ are lowest for An=Cm, there is not a discrete extreme in that parameter, but rather a gradual decline across the series (Figure S9). The elongation of the Cm-O_T bond in $CmO(OH)_2^+$ is particularly pronounced and distinct; for all other $AnO(OH)_2^+$, the An-O_T distance is similar to An-O_{YL} in $AnO_2(H_2O)^+$.

An additional peculiarity at curium is apparent in $AnO(OH)_2^+$ bond angles (Figure S10). In most cases the bond angle for $(OH)_{AX}$-An-O_T is within 20° of the linear 180° value, which is the rationale for loosely referring to this hydroxyl group as "axial". However, for An= Pa and An=Cm the deviation is much larger, with the two (OH) groups being equivalent such that there is no *TS-OH*. This equivalency of the two OH groups is also apparent from the distances in Figure 7, where An-$(OH)_{AX}$ and An-$(OH)_{EQ}$ are identical to one another for An=Pa and An=Cm (i.e. there is no *TS-OH*). The large deviation from a quasi-linear $(OH)_{AX}$-Pa-O_T geometry suggests a reduction in directional covalent bonding, or equivalently more ionic bonding character, for $PaO(OH)_2^+$.[30] It is similarly surmised that the actinide-oxygen bonding in far-from-linear $CmO(OH)_2^+$ is more ionic than in other $AnO(OH)_2^+$. Referring to the distances in Figure 7, we infer that loss of some covalent component of An-(OH) bonding results in bond elongation in $CmO(OH)_2^+$ relative to other $AnO(OH)_2^+$. The An-O_T bonds, like An-O_{YL} bonds, are expected to be more covalent than An-(OH) such that particularly drastic elongation of Cm-O_T as a result of reduced covalency is consistent with our assessment. This elongation is consistent with the NBO β spin density of 1.05 on the O_T. The amount of β spin density on O_T increases from 0.07 for U to 0.44 for Am before substantially increasing for Cm. The β spin density then drops to 0.04 for Bk. The β spin density on the (An)-O(H) is also maximized at Cm with a value of 0.24. QTAIM[46] charges were calculated using AIMALL[47] and are given in the SI. The charges show that the Cm in $CmO(OH)_2^+$ has the smallest positive charge among the An and that the (Cm-)O_T oxygen has the least negative charge. As reported previously,[30] another anomaly at curium for the series of $AnO(OH)_2^+$ is a clear minimum there in the 6d orbital population. This 6d depletion suggests a significant role for 6d orbitals in covalent An-O bonding that is disrupted in $CmO(OH)_2^+$; such a 6d contribution to bond covalency has also been suggested by Denning for actinyls.[20-21]

For oxidation states lower than An(V), stabilization due to electronic configurations with a half-filled $5f^7$ subshell can usually be predicted by treating the actinide as fully ionic. Accordingly, the particular stability of Cm(III) and Bk(IV) can largely be understood by considering them as free ions Cm^{3+} and Bk^{4+}, which both have configuration $[Rn]5f^76d^07s^0$.[48-49] However, oxides such as AnO_2^+ cannot reasonably be considered as bare An^{5+}, despite that the formal oxidation state is An(V). Instead, there is substantial electron donation from formally O^{2-} ligands to the central An^{5+} in $[O=An=O]^+$, which at least partly reflects covalent bond formation. Computed orbital populations (DFT NBO) for the species on the PES in Figure 1 were reported.[30]

Among all $AnO_2(H_2O)^+$ and $AnO(OH)_2^+$, the $CmO(OH)_2^+$ population, $[Rn]5f^{6.99}6d^{0.77}$, is closest to $5f^7$. The resultant charge on Cm is +2.28, which is well below the +5 charge for hypothetical fully ionic Cm(V). To attain the 5f population of 6.99, the corresponding 6d population of 0.77 is lower than for all other $AnO(OH)_2^+$. For $AmO(OH)_2^+$, for example, the 5f and 6d populations are 6.07 and 0.91, respectively. The $CmO(OH)_2^+$ species also has a distinctively high ratio for 5fα:5fβ electrons (6.69:0.30), which indicates only minor spin pairing, in accord with Hund's rule. We surmise that the peculiar properties of $CmO(OH)_2^+$, which relate to the propensity for oxo-exchange of curyl(V), might be traced to the special stability of the $5f^{6.99}$ configuration. Attaining a nearly "ideal" $5f^7$ configuration could modify the bonding in $CmO(OH)_2^+$ away from covalent and towards more highly ionic in character.

The equivalency of the two hydroxyl groups in $CmO(OH)_2^+$, as also in $PaO(OH)_2^+$, is consistent with the proposed enhancement in ionic character. In contrast, the non-equivalent hydroxyl groups in other $AnO(OH)_2^+$ presumably reflect directional covalent bonding character. The curium-oxygen bond elongations in $CmO(OH)_2^+$ may also be a manifestation of diminished covalency and/or enhanced ionicity. Notably, the charge q(Cm) in $CmO(OH)_2^+$ is evidently not anomalous in comparison with other q(An) in $An(OH)_2^+$, which suggests no distinctively diminished charge transfer from the oxygen atoms to curium. It should, however, be noted that aggregate charge transfer to a metal center alone is not necessarily a certain indicator of bond covalency. In particular, greater non-bonding (localized) character of electrons in the half-filled $5f^7$ subshell could inhibit covalency, without substantial moderation of the charge on the actinide center. Trends in bond distances in Figure 7, as well as other parameters not plotted, indicate that it is distinctively $CmO(OH)_2^+$ that exhibits bonding deviations, while CmO_2^+ falls in line with other AnO_2^+. It is reasonable that covalency is more rigorously imposed in curyl oxo-bonds than in typically ionic hydroxide bonds. Like the elongated ionic Cm-(OH) bonds, the Cm-O_T bond in the hydroxide is also substantially elongated relative to Cm-O_{YL} in curyl, which suggests that Cm-O oxo-bond covalency is disrupted in concert with that of Cm-$(OH)_{AX}$.

Bond critical points (BCPs)[46] were also calculated using the program system AIMALL (Supporting Information). The BCPs are closer to the O (~ 45%) than to the actinide (~ 55%) independent of the type of bond between the An and O. The variations in the BCPs are all within about 1%, except for the An=O bond where the variation is up to 3%.

CONCLUSIONS

AmO_2^+ and CmO_2^+ are remarkably abundant from ESI of Am^{3+} and Cm^{3+} solutions. Like other actinyl(V), AmO_2^+ and CmO_2^+ adsorb four waters in the gas phase. Reactions of $Am^{16}O_2^+$ and $Cm^{16}O_2^+$ with $H_2{}^{18}O$ reveal that AmO_2^+ does not oxo-exchange whereas CmO_2^+ does, confirming predictions. Because BDE[OAm^+-O] is lower than the BDEs for PaO_2^+ and UO_2^+, which do exchange, non-exchange of AmO_2^+ extends the disconnect between bond strength and reactivity. Given that oxo-exchange occurs by rearrangement, not cleavage, of actinide-oxo bonds the seemingly paradoxical result of more facile activation of stronger bonds is not necessarily incongruous.

Whereas PaO_2^+ and UO_2^+ oxo-exchange, this reactivity is absent for NpO_2^+, PuO_2^+ and AmO_2^+. The finding that CmO_2^+ does exchange confirms the predicted turn to higher reactivity from americyl(V) to curyl(V). A reevaluation of CCSD(T) results suggests that this reactivity turn is at least partly a manifestation of distinctive chemistry of Cm(V), with a striking elongation of the oxo-bonds in $CmO(OH)_2^+$. This peculiarity suggests relatively more ionic—and/or less covalent—character for the oxide hydroxide of curium(V) versus other actinide(V), which may relate to the Cm $5f^7$ configuration in $CmO(OH)_2^+$.

Oxo-exchange is sufficiently simple that trends can be understood though computational modeling. However, interrelated varying properties, such as simultaneous increases in ionic bonding and atomic charges,[30, 50] present challenges to understanding what effects actually govern reactivity. A key to advancement is studying multiple actinides; we have now experimentally assessed oxo-exchange for six actinyl(V) from PaO_2^+ to CmO_2^+. The demonstrated accord between experiment and theory provides confidence in computations for all AnO_2^+, as well as in inferences from these computations. The prospect of studying oxo-exchange of later actinyl(V), BkO_2^+, CfO_2^+ and/or EsO_2^+, is appealing but daunting given the very limited ($<10^{-7}$ g) available amounts of these heavy actinides.

Acknowledgements

This work was supported by the U.S. Department of Energy (DOE), Office of Science, Office of Basic Energy Sciences, Chemical Sciences, Geosciences, and Biosciences Division, Heavy

Element Chemistry Program, at Lawrence Berkeley National Laboratory under Contract DE-AC02-05CH1123 (TJ, PDD, DKS, JKG), at The University of Alabama (MV, DAD) through Grant No. DE-SC0018921, and at Washington State University through Grant No. DE-SC00085019 (KAP). D.A.D. thanks the Robert Ramsay Fund at The University of Alabama.

Associated Content

Geometrical parameters for the PES species; BCS Aimall; QTAIM Charges; PES to complete oxo-exchange; results for exposure to acetone (aco) for $AmO_2(H_2O)_2(aco)^+$ and $Am(OH)_2^+$; water addition to AmO^+ and CmO^+; oxo-exchange of CmO_2^+ after different times; oxo-exchange of AmO^+ and CmO^+; plots of E[*TS-PT*] and E[*TS-OH*], actinyl and An(V) hydroxide BDEs, and hydroxide bond angles $(OH)_{AX}$-An-O_T.

Table 1. Selected actinide-oxygen bond dissociation energies (BDEs in kJ/mol).[32]

An	An^+-O	OAn^+-O
Pa	800 ± 50	780 ± 29
U	774 ± 13	741 ± 14
Np	760 ± 10	610 ± 22
Pu	751 ± 19	509 ± 38
Am	560 ± 28	410 ± 56
Cm	670 ± 38	202 ± 60

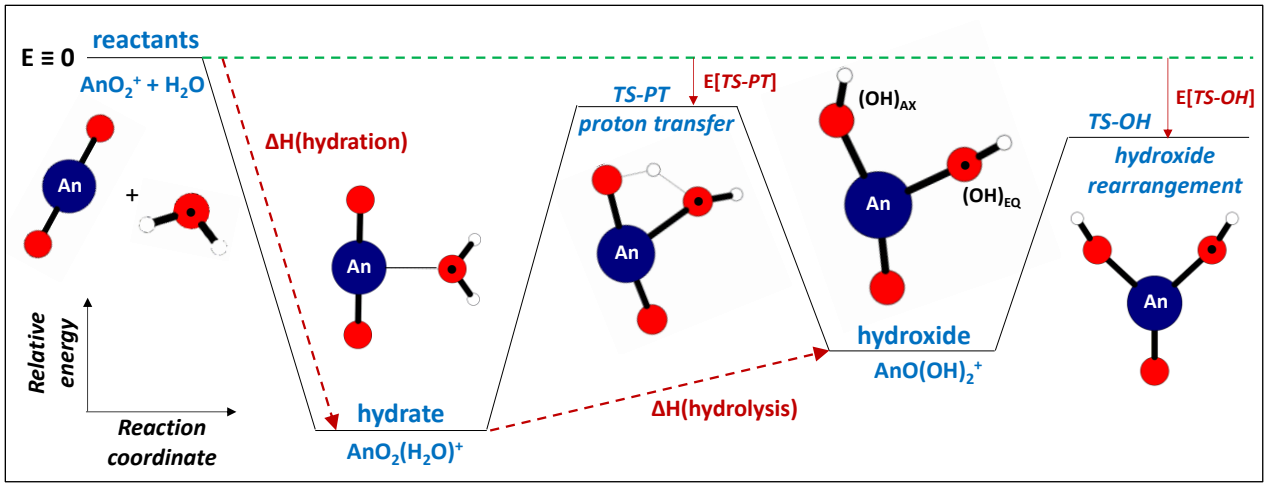

Figure 1. PES for reaction of $An^{16}O_2^+$ and $H_2{}^{18}O$; ^{18}O has a black dot. Separated reactants define zero energy; intermediates are physisorption hydrate and chemisorption hydroxide; transition states are for proton transfer, *TS-PT*, and hydroxide rearrangement, *TS-OH*. Oxo-exchange should occur if both E[*TS*]≤0. "Axial" $(OH)_{AX}$ and "equatorial" $(OH)_{EQ}$ become equivalent in *TS-OH*. Exchange to $An^{16}O^{18}O^+$ and $H_2{}^{16}O$ occurs by reversal on the PES from *TS-OH* (Figure S1). Exchange is predicted to occur when both *TS-PT* and *TS-OH* are below the energy of the reactants, as in the shown PES.

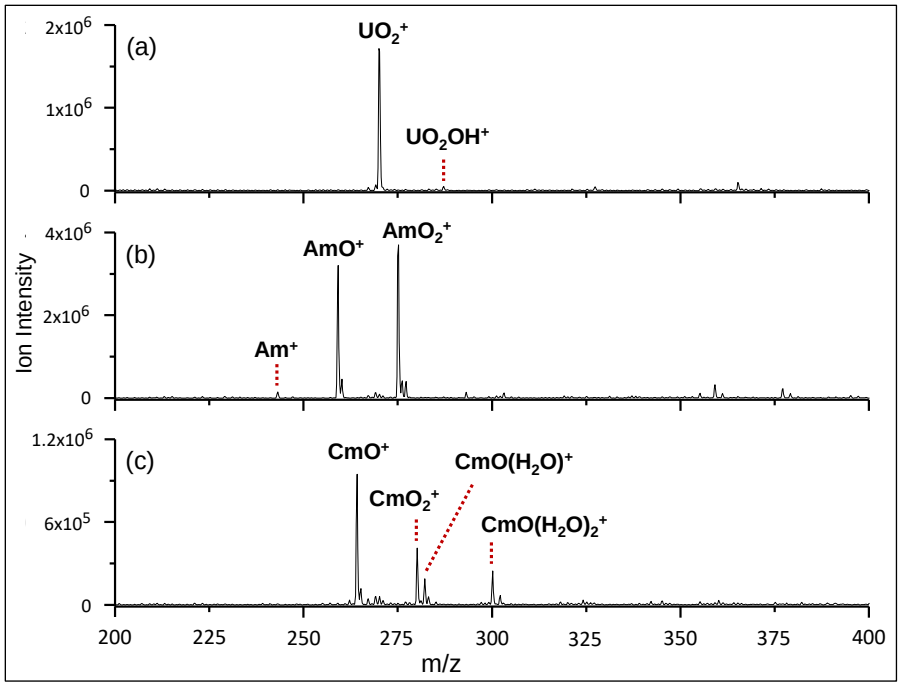

Figure 2. ESI mass spectra of solutions containing (a) UO_2Cl_2, (b) $Am(ClO_4)_3$, (c) $CmCl_3$. Peaks identified as hydrates $CmO(H_2O)^+$ and $CmO(H_2O)_2^+$ in (c) could instead be formulated as hydroxides $Cm(OH)_2^+$ and $Cm(OH)_2(H_2O)^+$, respectively.

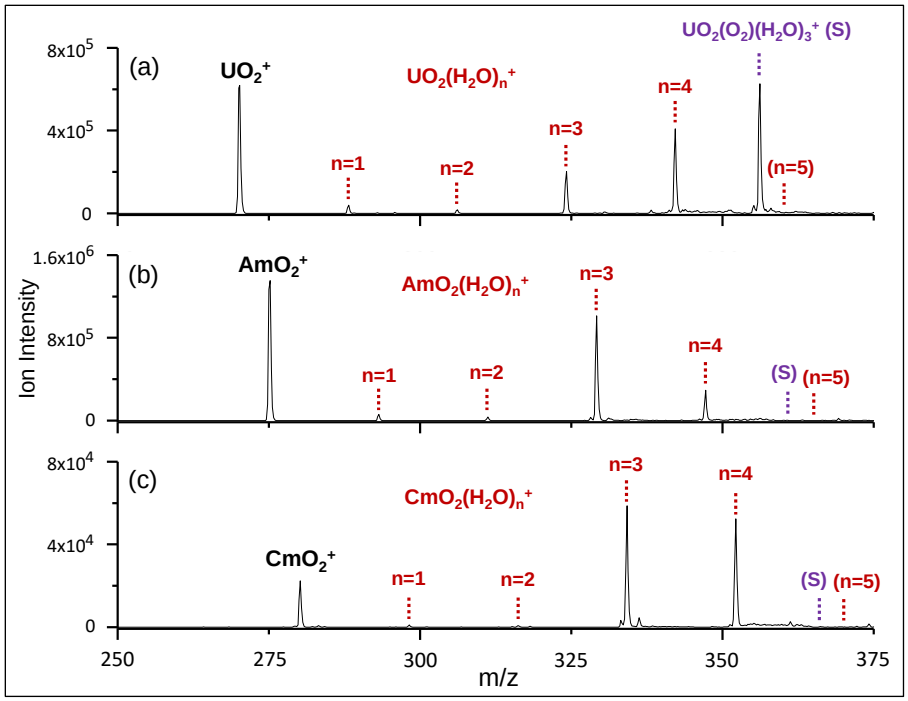

Figure 3. Mass spectra after 10 s reaction with background gases for (a) UO_2^+, (b) AmO_2^+ and (c) CmO_2^+. Addition of up to 4 H_2O is observed, with the non-observed 5th H_2O as indicated. Addition of H_2O to AnO_2^+ can result in $AnO_2(H_2O)^+$ or $AnO(OH)_2^+$; subsequent H_2O addition is by physisorbtion. After adjusting for P[H_2O] (~15% higher for CmO_2^+), relative rates the first H_2O addition are approximately 90:70:100 (UO_2^+:AmO_2^+:CmO_2^+). The results for UO_2^+, including O_2-addition to $U^VO_2(H_2O)_3^+$ to yield $U^{VI}O_2(O_2)(H_2O)_3^+$ (S) are as reported previously. Non-observed $AmO_2(O_2)(H_2O)_3^+$ and $CmO_2(O_2)(H_2O)_3^+$ would have appeared where indicated by "(S)".

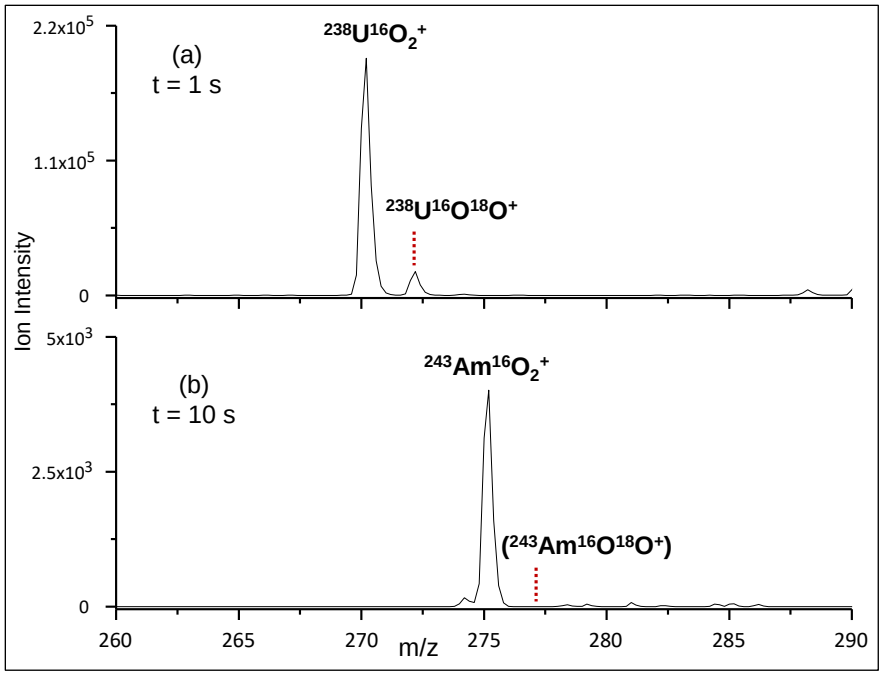

Figure 4. Mass spectra after exposure to $H_2{}^{18}O$: (a) $^{238}U^{16}O_2{}^+$ for 1 s; (b) $^{243}Am^{16}O_2{}^+$ for 10 s. Pressures of $H_2{}^{16}O$ and $H_2{}^{18}O$ are the same to within 10%. Non-detection of oxo-exchange for $AmO_2{}^+$ indicates exchange for $UO_2{}^+$ is at least 500x faster.

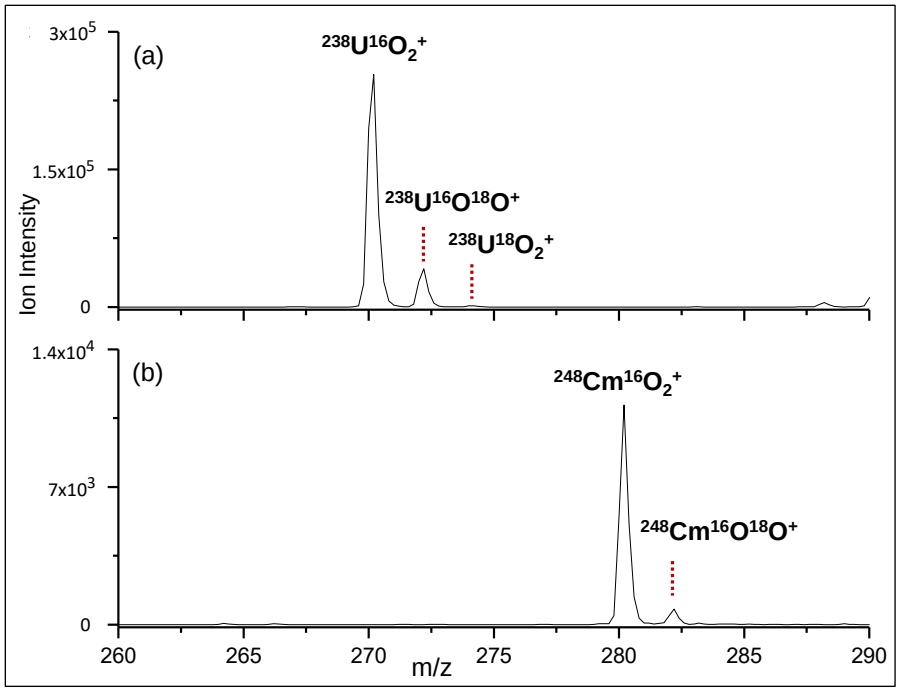

Figure 5. Mass spectra after exposure for 1.6 s to $H_2{}^{18}O$: (a) $^{238}U^{16}O_2{}^+$; (b) $^{248}Cm^{16}O_2{}^+$. Pressures of $H_2{}^{16}O$ and $H_2{}^{18}O$ are the same to within 10%. Oxo-exchange is roughly twice as fast for $UO_2{}^+$ versus $CmO_2{}^+$.

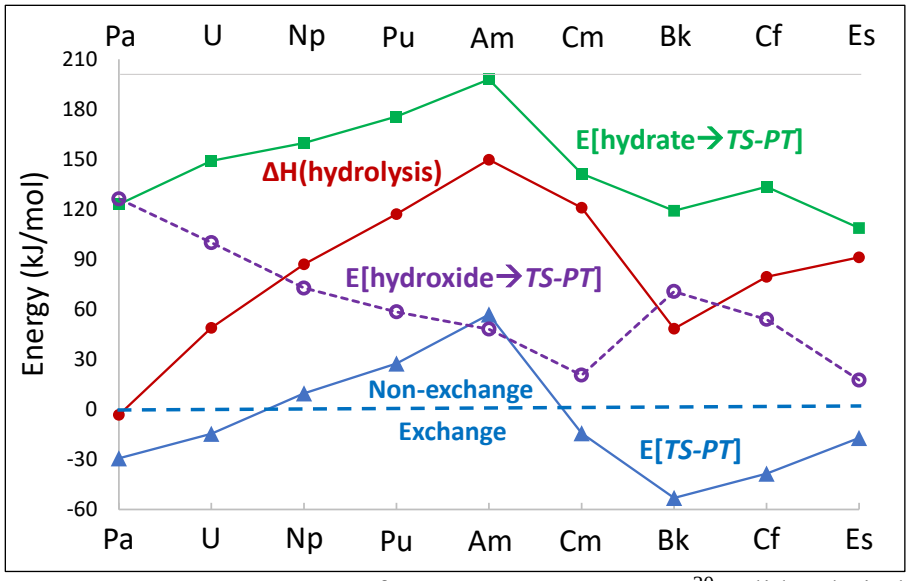

Figure 6. Selected energies for the PES in Figure 1:[30] solid red circles = ΔH(hydrolysis); solid green squares = E[hydrate→*TS-PT*]; open purple circles = E[hydroxide→*TS-PT*]; solid blue triangles = E[*TS-PT*]. Oxo-exchange is predicted if E[*TS-PT*] ≤ 0.

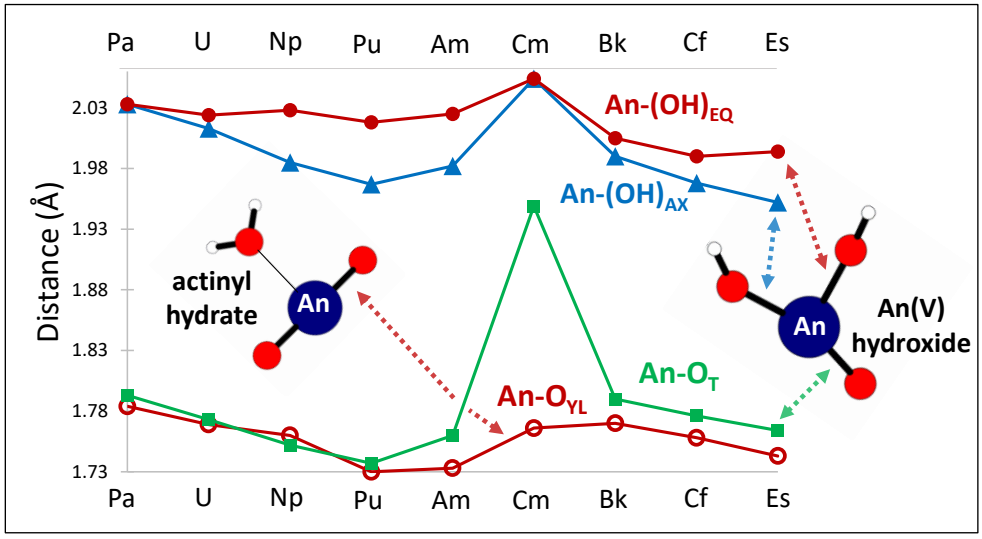

Figure 7. Computed An-O distances for hydrate and hydroxide intermediates on the PES in Figure 1.[30] An-O_{YL} distances are open red circles; hydroxide distances are terminal An-O_T (solid green squares), axial hydroxide An-$(OH)_{AX}$ (solid blue triangles), and equatorial hydroxide An-$(OH)_{EQ}$ (solid red circles).

References

1. Eller, K.; Zummack, W.; Schwarz, H., Gas-Phase Chemistry of Bare Transition-Metal Ions in Comparison. *J Am Chem Soc* **1990,** *112*, 621-627.
2. O'Hair, R. A. J., The 3D quadrupole ion trap mass spectrometer as a complete chemical laboratory for fundamental gas-phase studies of metal mediated chemistry. *Chem Commun* **2006**, 1469-1481.
3. O'Hair, R. A. J.; Rijs, N. J., Gas Phase Studies of the Pesci Decarboxylation Reaction: Synthesis, Structure, and Unimolecular and Bimolecular Reactivity of Organometallic Ions. *Accounts Chem Res* **2015,** *48*, 329-340.
4. Blagojevic, V.; Lavrov, V. V.; Bohme, D. K., Ligation kinetics as a probe for relativistic effects in ion chemistry: Gas-phase ligation of late atomic transition metal cations with OCS and CH3Cl at room temperature. *Int J Mass Spectrom* **2018,** *429*, 101-106.
5. Sabino, A. A.; Machado, A. H. L.; Correia, C. R. D.; Eberlin, M. N., Probing the mechanism of the heck reaction with arene diazonium salts by electrospray mass and tandem mass spectrometry (vol 43, pg 2514, 2004). *Angew Chem Int Edit* **2004,** *43*, 4389-4389.
6. Clemmer, D. E.; Aristov, N.; Armentrout, P. B., Reactions of ScO+, TiO+, and VO+ with D2 - M+-OH Bond-Energies and Effects of Spin Conservation. *J Phys Chem* **1993,** *97*, 544-552.
7. Dietl, N.; Schlangen, M.; Schwarz, H., Thermal Hydrogen-Atom Transfer from Methane: The Role of Radicals and Spin States in Oxo-Cluster Chemistry. *Angew Chem Int Edit* **2012,** *51*, 5544-5555.
8. Fiedler, A.; Kretzschmar, I.; Schroder, D.; Schwarz, H., Chromium dioxide cation OCrO+ in the gas phase: Structure, electronic states, and the reactivity with hydrogen and hydrocarbons. *J Am Chem Soc* **1996,** *118*, 9941-9952.
9. Waters, T.; Wang, X. B.; Wang, L. S., Electrospray ionization photoelectron spectroscopy: Probing the electronic structure of inorganic metal complexes in the gas-phase. *Coordin Chem Rev* **2007,** *251*, 474-491.
10. Clark, D. L.; Conradson, S. D.; Donohoe, R. J.; Keogh, D. W.; Morris, D. E.; Palmer, P. D.; Rogers, R. D.; Tait, C. D., Chemical speciation of the uranyl ion under highly alkaline conditions. Synthesis, structures, and oxo ligand exchange dynamics. *Inorg Chem* **1999,** *38*, 1456-1466.
11. Hayton, T. W., Metal-ligand multiple bonding in uranium: structure and reactivity. *Dalton T* **2010,** *39*, 1145-1158.
12. Arnold, P. L.; Pecharman, A. F.; Hollis, E.; Yahia, A.; Maron, L.; Parsons, S.; Love, J. B., Uranyl oxo activation and functionalization by metal cation coordination. *Nat Chem* **2010,** *2*, 1056-1061.
13. Arnold, P. L.; Pecharman, A. F.; Love, J. B., Oxo Group Protonation and Silylation of Pentavalent Uranyl Pacman Complexes. *Angew Chem Int Edit* **2011,** *50*, 9456-9458.
14. Jones, G. M.; Arnold, P. L.; Love, J. B., Controlled Deprotection and Reorganization of Uranyl Oxo Groups in a Binuclear Macrocyclic Environment. *Angew Chem Int Edit* **2012,** *51*, 12584-12587.
15. Moll, H.; Rossberg, A.; Steudtner, R.; Drobot, B.; Muller, K.; Tsushima, S., Uranium(VI) Chemistry in Strong Alkaline Solution: Speciation and Oxygen Exchange Mechanism. *Inorg Chem* **2014,** *53*, 1585-1593.
16. Szabo, Z.; Grenthe, I., Reactivity of the "yl"-bond in Uranyl(VI) complexes. 1. Rates and mechanisms for the exchange between the trans-dioxo oxygen atoms in (UO2)(2)(OH)(2)(2+) and mononuclear UO2(OH)(n)(2-n) complexes with solvent water. *Inorg Chem* **2007,** *46*, 9372-9378.
17. Gong, Y.; Vallet, V.; Michelini, M. D.; Rios, D.; Gibson, J. K., Activation of Gas-Phase Uranyl: From an Oxo to a Nitrido Complex. *J Phys Chem A* **2014,** *118*, 325-330.
18. Fortier, S.; Hayton, T. W., Oxo ligand functionalization in the uranyl ion (UO22+). *Coordin Chem Rev* **2010,** *254*, 197-214.
19. Clark, D. L.; Conradson, S. D.; Donohoe, R. J.; Gordon, P. L.; Keogh, D. W.; Palmer, P. D.; Scott, B. L.; Tait, C. D., Chemical Speciation of Neptunium(VI) under Strongly Alkaline Conditions. Structure, Composition, and Oxo Ligand Exchange. *Inorg Chem* **2013,** *52*, 3547-3555.

20. Denning, R. G., Electronic-Structure and Bonding in Actinyl Ions. *Struct Bond* **1992,** *79*, 215-276.
21. Denning, R. G., Electronic structure and bonding in actinyl ions and their analogs. *J Phys Chem A* **2007,** *111*, 4125-4143.
22. Crandall, H. W., The Formula of Uranyl Ion. *J Chem Phys* **1949,** *17*, 602-606.
23. Lang, S. M.; Fleischer, I.; Bernhardt, T. M.; Barnett, R. N.; Landman, U., Water Deprotonation via Oxo-Bridge Hydroxylation and O-18-Exchange in Free Tetra-Manganese Oxide Clusters. *J Phys Chem C* **2015,** *119*, 10881-10887.
24. Gordon, G.; Taube, H., The Uranium(V)-Catalysed Exchange Reaction between Uranyl Ion and Water in Perchloric Acid Solution. *J Inorg Nucl Chem* **1961,** *16*, 272-278.
25. Gordon, G.; Taube, H., The Exchange Reaction between Uranyl Ion and Water in Perchloric Acid Solution. *J Inorg Nucl Chem* **1961,** *19*, 189-191.
26. Rios, D.; Micheini, M. D.; Lucena, A. F.; Marcalo, J.; Gibson, J. K., On the Origins of Faster Oxo Exchange for Uranyl(V) versus Plutonyl(V). *J Am Chem Soc* **2012,** *134*, 15488-15496.
27. Dau, P. D.; Wilson, R. E.; Gibson, J. K., Elucidating Protactinium Hydrolysis: The Relative Stabilities of PaO2(H2O)(+) and PaO(OH)(2)(+). *Inorg Chem* **2015,** *54*, 7474-7480.
28. Trubert, D.; Le Naour, C.; Jaussaud, C., Hydrolysis of protactinium(V). I. Equilibrium constants at 25 degrees C: A solvent extraction study with TTA in the aqueous system Pa(V)/H2O/H+/Na+/ClO4-. *J Solution Chem* **2002,** *31*, 261-277.
29. Dau, P. D.; Vasiliu, M.; Peterson, K. A.; Dixon, D. A.; Gibson, J. K., Remarkably High Stability of Late Actinide Dioxide Cations: Extending Chemistry to Pentavalent Berkelium and Californium. *Chem-Eur J* **2017,** *23*, 17369-17378.
30. Vasiliu, M.; Gibson, J. K.; Peterson, K. A.; Dixon, D. A., Gas Phase Hydrolysis and Oxo-Exchange of Actinide Dioxide Cations: Elucidating Intrinsic Chemistry from Protactinium to Einsteinium. *Chem-Eur J* **2019,** *25*, 4245-4254.
31. Kovacs, A.; Dau, P. D.; Marcalo, J.; Gibson, J. K., Pentavalent Curium, Berkelium, and Californium in Nitrate Complexes: Extending Actinide Chemistry and Oxidation States. *Inorg Chem* **2018,** *57*, 9453-9467.
32. Marcalo, J.; Gibson, J. K., Gas-Phase Energetics of Actinide Oxides: An Assessment of Neutral and Cationic Monoxides and Dioxides from Thorium to Curium. *J Phys Chem A* **2009,** *113*, 12599-12606.
33. Rios, D.; Rutkowski, P. X.; Shuh, D. K.; Bray, T. H.; Gibson, J. K.; Van Stipdonk, M. J., Electron transfer dissociation of dipositive uranyl and plutonyl coordination complexes. *J Mass Spectrom* **2011,** *46*, 1247-1254.
34. Gronert, S., Estimation of effective ion temperatures in a quadrupole ion trap. *J Am Soc Mass Spectr* **1998,** *9*, 845-848.
35. Rutkowski, P. X.; Michelini, M. C.; Bray, T. H.; Russo, N.; Marcalo, J.; Gibson, J. K., Hydration of gas-phase ytterbium ion complexes studied by experiment and theory. *Theor Chem Acc* **2011,** *129*, 575-592.
36. Santos, M.; Marcalo, J.; Leal, J. P.; de Matos, A. P.; Gibson, J. K.; Haire, R. G., FTICR-MS study of the gas-phase thermochemistry of americium oxides. *Int J Mass Spectrom* **2003,** *228*, 457-465.
37. Gibson, J. K.; Haire, R. G.; Santos, M.; de Matos, A. P.; Marcalo, J., Gas-Phase Oxidation of Cm+ and Cm2+ - Thermodynamics of Neutral and Ionized CmO. *J Phys Chem A* **2008,** *112*, 11373-11381.
38. Mincher, B. J.; Schmitt, N. C.; Schuetz, B. K.; Shehee, T. C.; Hobbs, D. T., Recent advances in f-element separations based on a new method for the production of pentavalent americium in acidic solution. *Rsc Adv* **2015,** *5*, 27205-27210.
39. Rios, D.; Michelini, M. C.; Lucena, A. F.; Marcalo, J.; Bray, T. H.; Gibson, J. K., Gas-Phase Uranyl, Neptunyl, and Plutonyl: Hydration and Oxidation Studied by Experiment and Theory. *Inorg Chem* **2012,** *51*, 6603-6614.
40. Lias, S. G.; Bartmess, J. E.; Liebman, J. F.; Holmes, J. L.; Levin, R. D.; Mallard, W. G., Gas-Phase Ion and Neutral Thermochemistry. *J Phys Chem Ref Data* **1988,** *17*, 1-861.

41. Rutkowski, P. X.; Michelini, M. D.; Gibson, J. K., Proton Transfer in Th(IV) Hydrate Clusters: A Link to Hydrolysis of Th(OH)(2)(2+) to Th(OH)(3)(+) in Aqueous Solution. *J Phys Chem A* **2013,** *117*, 451-459.
42. Vasiliu, M.; Peterson, K. A.; Gibson, J. K.; Dixon, D. A., Reliable Potential Energy Surfaces for the Reactions of H2O with ThO2, PaO2+, UO22+, and UO2+. *J Phys Chem A* **2015,** *119*, 11422-11431.
43. Hammond, G. S., A Correlation of Reaction Rates. *J Am Chem Soc* **1955,** *77*, 334-338.
44. Edelstein, N. M.; Fuger, J.; Katz, J. J.; Morss, L. R., Summary and Comparison of Properties of the Actinide and Transactinide Elements. In *The Chemistry of the Actinide and Transactinide Elements*, Third ed.; Morss, L. R.; Edelstein, N. M.; Fuger, J., Eds. Springer: Dordrecht, The Netherlands, 2006; Vol. 3, pp 1753-1835.
45. Lumetta, G. J.; Thompson, M. C.; Penneman, R. A.; Eller, P. G., Curium. In *The Chemistry of the Actinide and Transactinide Elements*, Morss, L. R.; Edelstein, N. M.; Fuger, J., Eds. Springer: Dordrecht, The Netherlands, 2006; Vol. 3, pp 1397-1443.
46. Bader, R. F. W., *Atoms in Molecules: A Quantum Theory*. Clarendon Press: Oxford, 1990.
47. Keith, T. A. *AIMAll*, 17.01.25; Gristmill Software: Overland Park, Kansas, 2017.
48. Heathman, S.; Haire, R. G.; Le Bihan, T.; Lindbaum, A.; Idiri, M.; Normile, P.; Li, S.; Ahuja, R.; Johansson, B.; Lander, G. H., A high-pressure structure in curium linked to magnetism. *Science* **2005,** *309*, 110-113.
49. Deblonde, G. J. P.; Sturzbecher-Hoehne, M.; Rupert, P. B.; An, D. D.; Illy, M. C.; Ralston, C. Y.; Brabec, J.; de Jong, W. A.; Strong, R. K.; Abergel, R. J., Chelation and stabilization of berkelium in oxidation state plus IV. *Nat Chem* **2017,** *9*, 843-849.
50. Kaltsoyannis, N., Covalency hinders AnO(2)(H2O)(+) -> AnO(OH)(2)(+) isomerisation (An = Pa-Pu). *Dalton T* **2016,** *45*, 3158-3162.

For Table of Contents Only

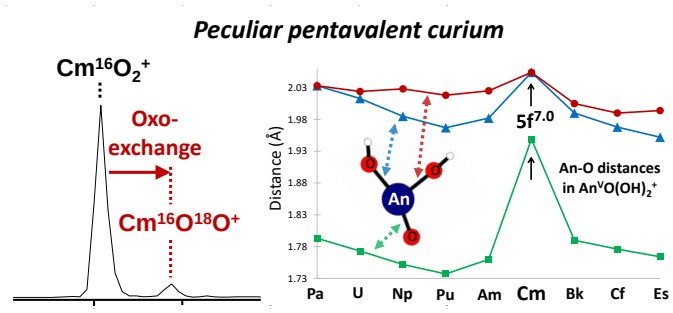

Reactivity trends across the actinide series provide fundamental insights. Exchange of an oxygen from water with one from an actinide(V) dioxide cation requires An-O bond activation. We previously observed oxo-exchange for PaO_2^+ and UO_2^+, but not NpO_2^+ and PuO_2^+. We here report oxo-exchange for CmO_2^+, but not AmO_2^+. The reactivity increase from Am(V) to Cm(V) reveals distinctive curium behavior that may be related to filling of the 5f electron subshell.